**Misan Journal of Engineering Sciences** ISSN-E: 2957-4250
Vol. 4, No. 2, Dec 2025 ISSN: 2957-4242

# Effect of heating elements types on air preheater performance: Review

Saad H. Saadon[1,2,*], Mohammed H. Alhamdo[2]

[1] *Department of Mechanical Engineering, University of Misan, Misan, Iraq*

[2] *Department of Mechanical Engineering, Mustansiriyah University, Baghdad, Iraq.*

**Corresponding author E-mail: ehph023@uomustansiriyah.edu.iq*

*(Received 30 June, Revised 3 Oct, Accepted 3 Oct)*

**Abstract:** In the air conditioning, steel industry, and power plants, rotating heat exchangers are utilized to preheat air for use in waste heat recovery or steam generators. In this article, various rotating heat exchangers that are utilized in thermal power plants have been presented to preheat the air supplied to the steam generators. The heat transfer between two fluid streams is accomplished in these devices via a rotating matrix that functions as a thermal accumulator by alternatingly coming into contact with the two fluid streams. Although a considerable number of studies have investigated the influence of types of heating elements on the performance of air preheaters, there is a scarcity of exhaustive review articles that encompass the latest developments in this domain. This paper provides a comprehensive review of recent available studies that investigate the impact of flow configuration, material, and geometry of the heating elements on the air preheater thermal hydraulic performance. It found that the replacement of the air preheater's baskets with new ones featuring distinct profiles increased the heat transmission rate. Also, the resistance coefficient and Nusselt number increased in tandem with the corrugation angle. The heat regeneration temperature and the heat exchanger's efficiency were observed to decrease as the matrix's rotating speed and the hot flow's mass flow rate increased, according to the results.

**Keywords:** Heating elements, Air preheater, power plants, Heat transfer, Thermal efficiency

## 1. Introduction

The majority of steam-generating facilities contain air preheaters, which function to elevate the combustion air temperature and improve the overall combustion process. The majority of applications utilize flue gas as the primary energy source, while the air preheater functions as a heat reservoir, capturing and transferring thermal energy from the flue gas to the incoming air [1] The idea proposes that preheating the primary air acts as a catalyst for grate ignition rather than just drying the trash [2]. Primarily, two categories of air preheaters exist according to their operating principle. Recuperative and regenerative. Moreover, regeneration was separated into stationary and rotating. The recuperation process was separated into tabular and plate types [3]. The rotary air preheater, one of the techniques utilized in steam-based power plants to recover critical energy, was implemented by Ljungstrom in 1920. Due to its compact volume, light weight, flexible design, and lower risk of low temperature corrosion as compared to a uniform air preheater, the rotary type has been widely utilized[4]. An energy transmission occurs between hot stream fluid and cold fluid through the utilization of a rotating matrix composed of densely packed space plates [5].Figure 1 the composition of a RAPH, which is a component utilized in power plants that use coal. It consists of segmental plates, beams, gas channels, and sector gaskets.

DOI: https://doi.org/10.61263/mjes.v4i2.176

The matrix of the rotor consists of enormous heat-transfer elements. Heat is continuously transferred from the heated flue gas to the matrix in the sector of gas and from the matrix to the cooled air in the sector of air as the rotor rotates slowly [6].

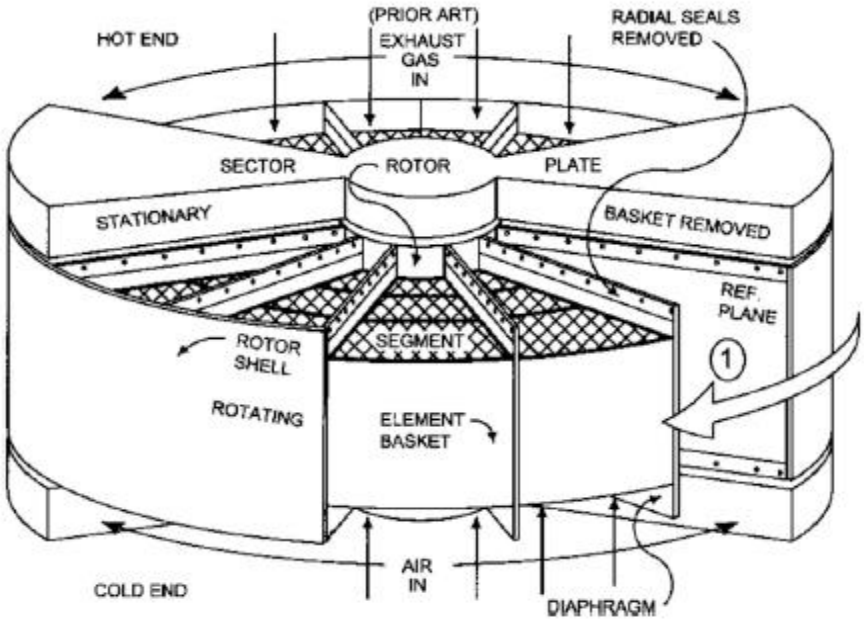


Figure 1. diagram of the rotary air preheater [6]

When assessing the performance and longevity of rotary preheaters, three critical factors must be considered: thermal performance, leakage, and corrosion. The thermal performance of rotary preheaters can be assessed by examining the heat transfer and temperature distribution in the heating elements. Leakage, in particular, has the potential to compromise thermal performance and contribute to corrosion. Corrosion influences the lifespan of thermal elements concurrently [7]

The ensuing literature comprises research articles that examine the thermal elements component. While numerous studies have examined the impact of heating elements on the efficiency of air preheaters, there is a dearth of comprehensive review articles that cover the most recent advancements in this field. While Modi et al. [8] produce a review article on heat transfer elements; they omit a number of the papers. In addition, the research methodology was not explicitly stated. The CFD analysis for the rotary air preheater was incorporated by Patel et al. [9] without taking into account the other studies . Rajan et al.'s research [10] has focused on tri-sector air preheaters (APH). The study employed the model to compute the temperature distributions and pressure drop at the air preheater's flue gas exit. Baruah and Kumar [11] have highlighted several developments in the numerical modeling of regenerative rotary heat exchangers in respect to fluid flow and heat transfer. Also stated that, commercially available CFD codes are used by a number of industries to simulate fluid flow and heat transfer as well as to research increased heat transfer. The most often utilized codes among them are FLUENT, CFX, STAT-CD, FIDAP, PHOENICS, ADINA, and CFD2000.

This review integrates and synthesizes the current body of knowledge on how heating-element types affect air-preheater (APH) performance. It provides a comprehensive overview of primary studies and their collective findings while noting that, despite many individual investigations of heating elements and APH efficiency, recent comprehensive reviews remain scarce. In response, the review specifically focuses on how element

surface topology, material selection, and geometric configuration influence heat-flux distribution and overall thermo-hydraulic performance within the APH. It identifies research gaps, highlights inconsistencies among prior results with plausible explanations, and critically appraises study quality by evaluating the strengths, limitations, and methodological choices in both experimental and computational work. It situates the topic in its historical and conceptual context, proposes practical methodological guidance and a unifying framework to reconcile divergent evidence, and outlines a clear research agenda with specific, testable questions and hypotheses to advance design and evaluation practice and to help newcomers get up to speed efficiently.

## 2. Element surface

Early works such as Stasiek [12]and Ciofalo et al. [13] focused on **cross-**corrugated plate heat exchangers, reporting that large-eddy simulation (LES) models yielded the most accurate predictions of Nusselt number and friction factor when compared with experiments. At the laboratory scale, Ghodsipour [14] employed triangular matrix regenerators and conducted ANOVA analysis, finding efficiencies ranging from 0.58 to 0.975. Zhang and Che [15] examined double notched plates, demonstrating up to ±17% deviation in CFD-predicted Nu and j-factors compared with experiments. An intriguing study by Sivageerthi et al. [16] proposes to figure out and assess the important elements that must be addressed in order to improve the coal-fired thermal power plant (CTPP) performance. Twenty-four critical factors are identified through a survey of the literature and industrial interactions. The important factors are ranked using the fuzzy analytic hierarchy process (FAHP), and the relationships between the important factors are revealed using the fuzzy decision-making and trial laboratory (FDEMATEL). The first step of the study is devoted to identifying and compiling a list of factors influencing the performance of CTPPs. After accumulating the factors influencing the performance of the CTPP, the factors are assessed in order to determine their priority and establish their relationship. Experts were tasked with conducting pairwise comparisons of the factors. Experts calculate the relative weight of each factor's significance. According to this study, the heating element profile's relevance ranks sixth among the 24 factors which means the importance of the geometry of the heating elements. Bu et al. [17] introduced a split regenerative APH with double-undulated (DU) versus DU3E elements, achieving a 90% reduction in ammonium bisulfate (ABS) deposition with payback times of less than two years.

Jordan White and Marco Vezza [18] have effectively modeled and validated experimentally and numerically (STAR-CCM+ CFD) a Flat Notched Crossed plate. The effect of varying the Flat-Notched-Crossed's pitch and radius element plate on heat transfer and pressure drop characteristics was evaluated. It was discovered that both variables substantially affected the element's performance. While it is generally accepted that a larger surface area facilitates greater heat transmission, it found that vortices and turbulence control are significant design performance factors. This study seeks to optimize the element plate in the Flat Notched Crossed (FNC) style using CFD techniques by changing its geometric dimensions. Modern optimization techniques typically employ surrogate modeling to precisely identify the optimal solution. Constructing a function to roughly represent the relationship between the variables (inputs) and the outputs (results) is a potent aspect of surrogate modeling. Response Surface Methodology (RSM) and Kriging are the two most prevalent surrogate modelling methods. RSM approximates the correlation with a polynomial function. Kriging employs a global polynomial model in conjunction with a covariance matrix to account for local deviations. The authors then employed Kriging with the MATLAB DACE utility. They conclude that: The optimized Flat Notched Crossed design enhances heat transfer and decreases pressure drop. The primary driver of enhanced heat transfer is turbulence. Certain elements contribute minimally to the heat transfer.

Bureska and Bundalevski [19] showed that the 30% expansion of the heating surface and replacement of the baskets in the regenerative air preheater are among the measures to reduce the temperature of the flue gas. The profiles of the plates in the new baskets diverge from the old ones. The old "N" profile from the first two levels has been supplanted with the "DU" profile. In the intermediate and cold levels, "NF" profile is replaced the old profile. Replacement of the air preheater's baskets with new ones featuring distinct profiles increased the heat transmission rate while lowering the flue gas temperature from $207^0$C to $191^0$C. Reducing the flue gas

temperature by 100 degrees' Celsius increases boiler efficiency by 0.8 percent and decreases coal consumption by 0.83 percent.

Gulluce and Ozdemir[20] showed theoretically that by just updating the existing matrix profile, a significant amount of efficiency might be enhanced at a bearable cost penalty. Notched Undulated (NU) with corrugated-undulated elements (CU), as illustrated in Figure 2. It is concluded that, as a result of optimized CU, and Rotary Regenerative Heat Exchanger (RHEX) shape as well as the angular velocity, by simply substituting the current matrix profile with CU elements, RHEX effectiveness can be increased by 92% at a cost of 66%. Furthermore, the cost may be reduced by 46.11%, the efficiency increased by 32.02%, and the entropy generation number reduced by 16.60%. There were two optimization issues taken into consideration: the first is the optimization of the current design by substituting CU plates for the matrix elements, and the second is the optimization of the design and operational conditions to design RHEX under the same boundary conditions, such as inlet temperatures and mass flow rates using CU plates. For improved turbulence characteristics, greater values of sinusoidal pitch, inner height, and undulation angle of the undulated plate are preferred. Similarly, increasing the length of the matrix is required to increase the fluid's residence time and the heat transfer area. Yu et al. [21] examine the effects of the enamel heat storage element's corrugated angle and width on flow and heat transfer efficiency as illustrated in Figure 2. Upon varying the corrugation inclination (θ) and ripple width (b), the following outcome was observed: as the corrugation angle increased, so did the resistance coefficient and Nusselt number. Both the resistance coefficient and the Nusselt number rise as the heat storage element's ripple width does. There could be a noticeable inaccuracy with assumptions like constant wall temperature and zero wall thickness of the heating storage. Wei et al. [22] made assumptions by modeling an air preheater's interior circulation unit and only accounting for half of the wall thickness in their computation. Numerical investigation using ANSYS Fluent has been used to study the temperature distribution in the heat storage elements.

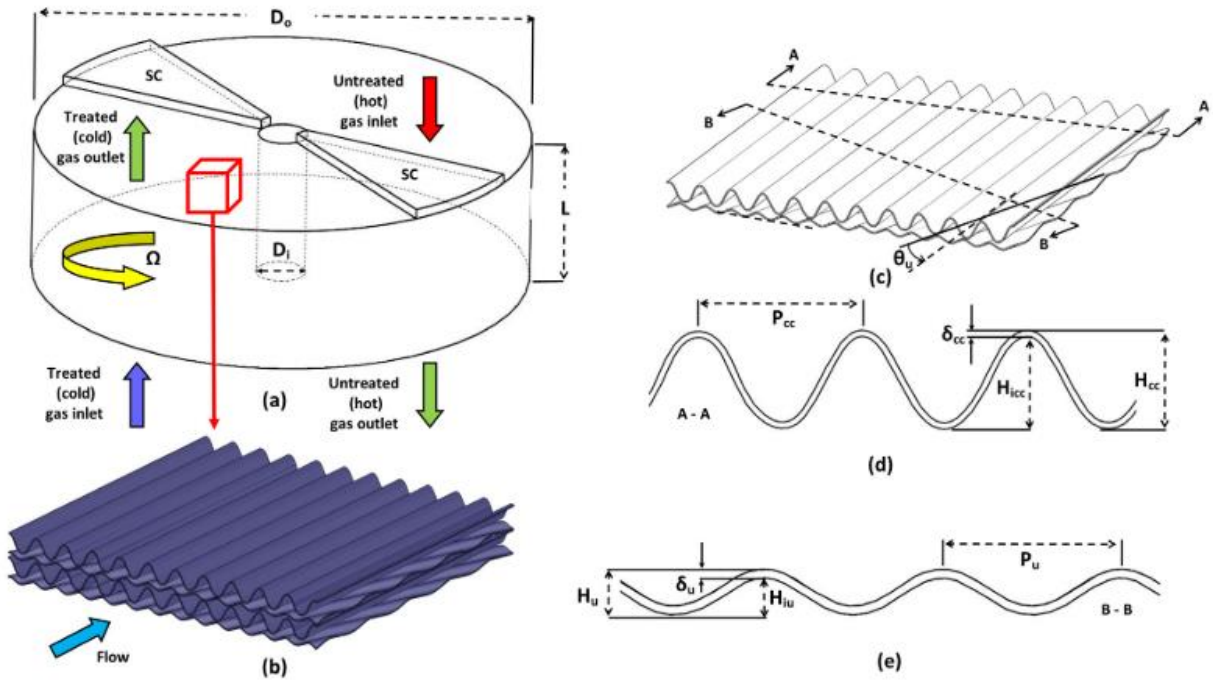


Figure 2. (a) Schematic diagram of the APH (b) Heating element (c) profile of corrugated and undulated plates (d) cross section of corrugated plate), and (e) cross section of undulated plate [15]

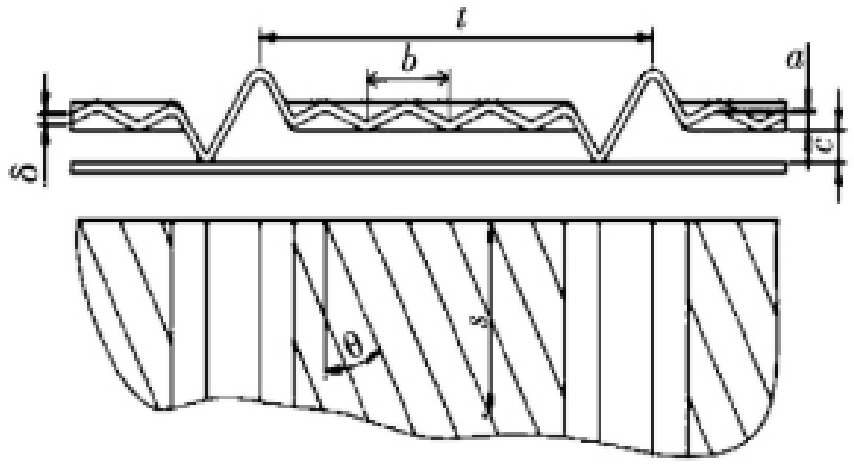


Figure 3. Corrugated plate profile [16]

The authors were unable to locate any research that takes into account different thermal surfaces when simulating the power plant's rotating regenerators (i.e., by accounting for typical surfaces in Ljungstrums). This void was identified by H. Abroshan and M. Goodarzi[23] .To accomplish the greatest fuel savings, the rotating speed and size of hot, intermediate, and cold end layers were optimized. These specifications comprised hydraulic diameters, heating profile type, and layer length. Results indicated that CU, FNC, and DU perform better at low Reynolds numbers. As Reynolds increased, the efficiency of FNC decreased dramatically. From a thermal transfer perspective, CU and then DU performed significantly better than DU. Despite the fact that corrugated undulated (CU) is the ideal heating surface for all Reynolds numbers, as shown by $Nu/f^{1/3}$ graphs for different flow channels considered, in the majority of optimization sets, for hot and intermediate layers, Flat Notched Crossed (FNC) was recommended. Due to the convenience of cleaning, only two passages were considered for the cold end: notched flat (NF) and straight corrugated plate (CP). In the majority of instances, the NF was chosen by the optimization algorithm

Five heating-element profiles were examined by Patel et. al. [24]. They were: (1) Corrugated undulated; (2) Notched flat; (3) Notched corrugated; (4) Double undulated; and (5) Advanced clear element. An optimization and CFD study of the profile elements of the Ljungstrom air-preheater demonstrated that.

1) The element profile primarily determines how much heat is exchanged in an air preheater.

2) The Advanced Clear Element (ACE) model performs well when compared to the air and hot flue gas outlet temperatures.

Manivel et al. [25] modify the profile by replacing the 0.8 mm DU profile with 1.2 mm thick NF components. This increases the heat transfer area and lowers the flue outlet temperature by $40^0$C, resulting in a 0.2% increase in efficiency.

By altering the height of the hot, intermediate, and cold layers, the overall weight of the heating elements has been reduced, as proposed by Wang et. al. [26]. The suggested design was 0.3, 0.3, and 0.684 in height, whereas the original height was 0.45, 0.9, and 0.7, respectively. When compared to the original design, the total weight of the heat transfer elements was lowered by at least 26.5%. RAPH's capital cost might be significantly lowered.

The geometry of the heating element was optimized by Lee et al. [27] in order to effectively reduce differential pressure and enhance performance. The thermal fluid properties of the heating component and Gas- Gas

Heater(GGH) system were investigated in order to determine the pitch, plate angle, and undulated angle. Pressure drop is reduced as the undulated angle and pitch increase by increasing the heating element's cross section, as determined by the optimization result. The performance of the GGH is improved by increasing the plate angle because it secures the heat transfer area and compensates for the decreased heat transfer coefficient.

For corrugated undulated (CU) heat transfer surfaces, to achieve a maximum heat transfer capacity and a low pumping power, as illustrated in Figure 4, a multi-objective genetic algorithm was used by Wang et al. [28] using the Pareto optimum technique to get the ideal values for the pitch and height of the corrugated plate (C-plate) and the undulated plate (U-plate). Using three-dimensional numerical simulations, investigations were conducted into how geometrical parameters affected the thermo-hydraulic effectiveness of the CU heat transfer surface. When the Reynolds number changed from 1,500 to 10,000, the principal findings can be summed up as follows:

(1) Due to the principal flows' frictional effect in the C-plate channel and the U-plate channel, intense secondary flows occurred in both channels. Thus, the heat transfer surfaces and bases of the C- and U-channels might receive the cold flow that is directed toward them from the passage's center.

(2) While an increase in $H_U$ would result in more turbulence and mixing in the flow, an increase in $P_U$ would decrease the frequency of U-plate disruptions to the primary flow. However, if the $P_U/H_U$ ratio was held constant, the change in $H_U$ would have a greater influence on the U-plate's perturbation influence than that of $P_U$.

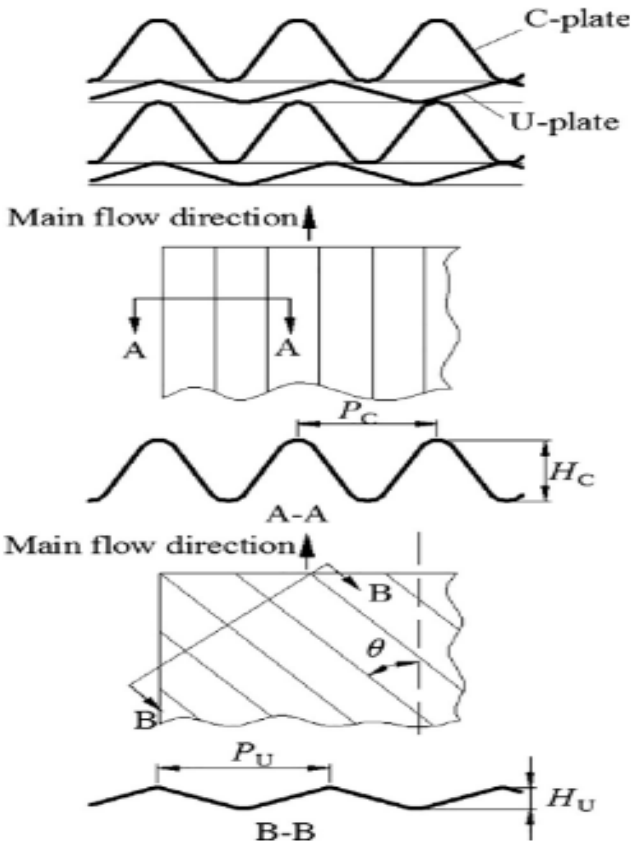


Figure 4. Corrugated-undulated heating elements presented in [23].

Mallikarjuna et al.[29] show that the 1.2 mm thick NF profile elements that are standard on old air pre-heaters can be switched to 0.8 mm DU profile in the cold end baskets. Due to this, the temperature of the flue gas exit will drop as the heat transfer area grows. A periodic flow regenerated APH's unsteady energy model, both experimental and numerical, is described. The considerable thermal influence of the basket walls enclosing the heating element matrices is being developed by Ghanim K. and Alhamdo [30]. Five types of plates were used: parallel to the direction of flow, corrugated plate, (CP), corrugated plate with ($\theta = 15^0$, $\theta = 30^0$, $\theta = 45^0$) and flat plate, (FP). By combining the five plate types listed above, it is possible to generate seven geometric configurations that can function as heat transfer matrices for APH. Variations are seen to be introduced when basket wall surfaces are present in matrix and fluid temperatures across a given cross-section. The temperatures near the wall differ substantially from those in the center. The basket wall is designed to induce a unique thermal response for each tested material type. Consequently, ignoring the basket walls effect may result in grave errors. The experimental setup plate is given in Figure 5.

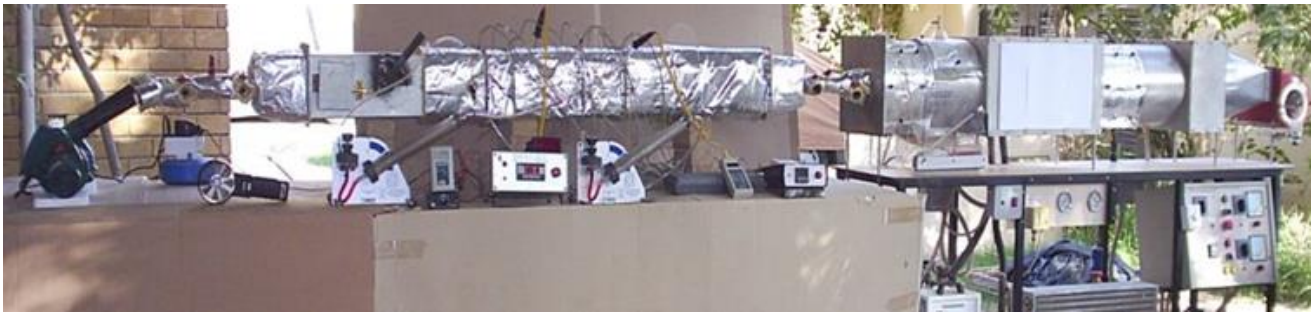

Figure 5. Experimental setup plate used in [25]

For the J-factor to precisely estimate a suitable temperature distribution within APH matrices across a range of Reynolds numbers, new (13) correlations were derived.

The matrix metal experiences continual thermal fatigue stress as a result of the temperature differential between the heating and cooling cycles. Determining the thermal fatigue stresses is essential in various regions of the APH in order to predict the likelihood that one region will fail before another, as suggested by Vulloju et al. [31]. Cold flow experiments are used to analyze two types of element profiles: flat notched crossed and double undulated elements in a wind tunnel and their performance at various Reynolds numbers is compared. The efficiency of heat transfer elements is evaluated using two tests, Residual Time Test and Cold Flow Studies. The diagnostic result indicates;

1) The performance of DU and FNC elements is shown to be mostly unaffected by hydraulic diameter because there is little variation in hydraulic diameter between DU and FNC elements.

2) The pair height of FNC elements is smaller than that of DU elements. In a given number of element pairings, FNC elements occupy less volume than DU elements. Consequently, the size and weight of the APH can be reduced by substituting DU elements with FNC elements. 3) It is determined that the heat transfer coefficient of FNC elements is greater than that of DU elements because the residual time of FNC elements exceeds that of DU elements. 4) The fluid pumping capacity is proportionate to the fluid across element pressure drop. FNC element have less fluid pumping capacity compared to DU elements.

With very minor modifications to the heat exchanger surfaces' shape, the increase in matrix heat capacity was investigated by Stupar et al. [32]. Simultaneously, the impact of reduced air leakage via the seals on the efficiency of the facility was examined. Small variations in undulation height result in considerable changes in features of heat exchange. As a result, the height of undulation throughout this research was modified within the tight limitations allowed, as illustrated in Figure 6. For minimum changes to the geometry of the matrix

sheets, an increase in the heating surface of the air preheater was explored. The improvements represented enabled an increase in the rotary regenerator matrix mass, and hence its heat capacity. Analysis revealed that increasing the matrix heat capacity under identical air infiltration conditions in the steam boiler invariably leads to increased efficiency of the air preheater and the steam boiler. Constructed optimization approaches introduced by Hajabdollahi [33] lead tom improve effectiveness by 7% while reducing total annual cost by 34%.

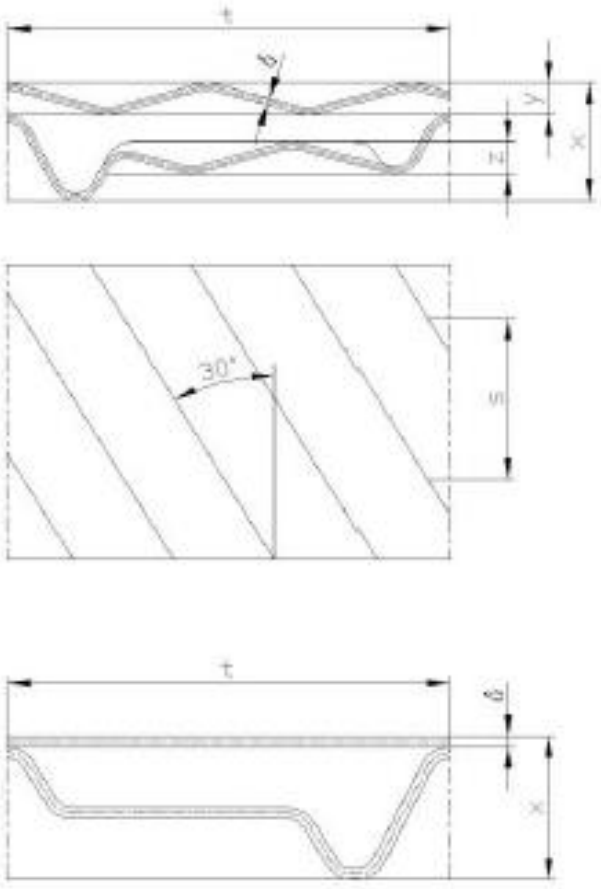


Figure 6. Geometry of heating elements: double undulating in the upper right and notched plain on the lower right [27]

## 3. Element material

In terms of mechanical reliability, Wang [34] quantified stress and deformation in APH elements, reporting small discrepancies (1–5%) between simplified numerical models and experiments. Ngo et al. [35] computed and contrasted the thermal performance of APH composed of different materials with different flow channel and matrix wall thicknesses. Due to its lightweight design, and robust resistance to corrosion, a polymer rotary regenerator can reduce the operating costs, and maintenance requirements of a thermal system. To assess the viability of using polymers in an air-preheater of a thermal power plant, the thermal performance of APH was numerically studied using ANSYS Fluent based on the thicknesses of the flow channel, matrix, and matrix material. Aluminum, polytetrafluoroethylene (PTFE), polyether ketone (PEEK), and corrosion-resistant low-alloy steel (CRLS) flat-plate type APH were taken into consideration. Polymer materials, as opposed to traditional metal materials, can be used as an APH matrix materials without significantly lowering its thermal

performance. If an appropriate additive could be added to PTFE or PEEK to create a matrix for an APH, its effectiveness would be on par with or even higher than that of metal APH s found in traditional TPPs.

Several air preheater matrix models have been investigated and contrasted by S. M. Hazim and M. H. Alhamdo[36] utilizing the conventional air preheater matrix model so as to replace the final basket of the original matrix with a material resistant to corrosives in the new matrix and to increase the pressure drop and the heat transfer rates of the matrix by adding a bypass tube with an appropriate ratio. The experimental work, as illustrated in Figure 7, of model of air preheater with periodic flow has been analyzed to determine the optimal factor of performance.

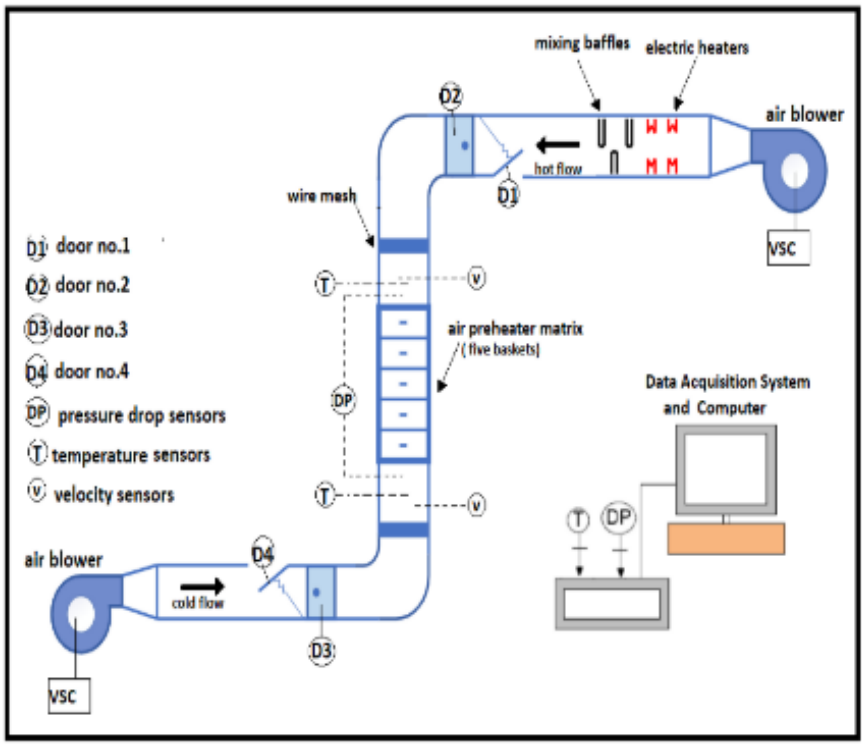


Figure 7. Schematic diagram of the experimental rig suggested by [29]

Based on the evidence, it is possible to draw a few findings:

Similar to the (P matrix) model, the (P+CG) model offers a high pressure drop and the similar rates of heat transmission.

Using the (P+CG+Ts) and (P+CG+Ti) models, the bypass tubes raise the heat transfer rate (Qav.) by 22% and 16%, respectively, in comparison to the (P matrix) model.

Heat transfer quantity per unit volume and the temperature differential between the heating surface and the working fluid are measured by Zhang et al.[37]. Numerical results indicate that the variations in heat transfer performance between the cold and hot ends are due to different materials and types of heating surfaces. The scouring velocity varies because of variations in the volumetric flow rate caused by temperature differences in the working fluid between the hot and cold ends.

Wang et al. [38] compared the flow and heat transfer efficiency of honeycomb ceramic and metal corrugated plates in rotary air preheaters. The influence of flue gas velocity and switching time on APH flow and heat

transfer efficiency was investigated. They presented an experimental (Figure 8) method for obtaining experimental correlations between convective heat transfer and the efficiency of rotational air preheaters that do not rotate the heat transfer elements. As the transition time increased, the outlet-air temperature, thermal effectiveness, and air-side pressure drop decreased, whereas the flue-gas pressure drop increased.

The output air temperature and effectiveness rose as the flow velocity increased; nevertheless, the pressure decreases of both air and flue gas increased. The rotary air preheater with corrugated metal plates had a higher outlet air temperature, greater efficiency, and a lower pressure drop under the same experimental conditions as the rotary air preheater with honeycomb ceramics.

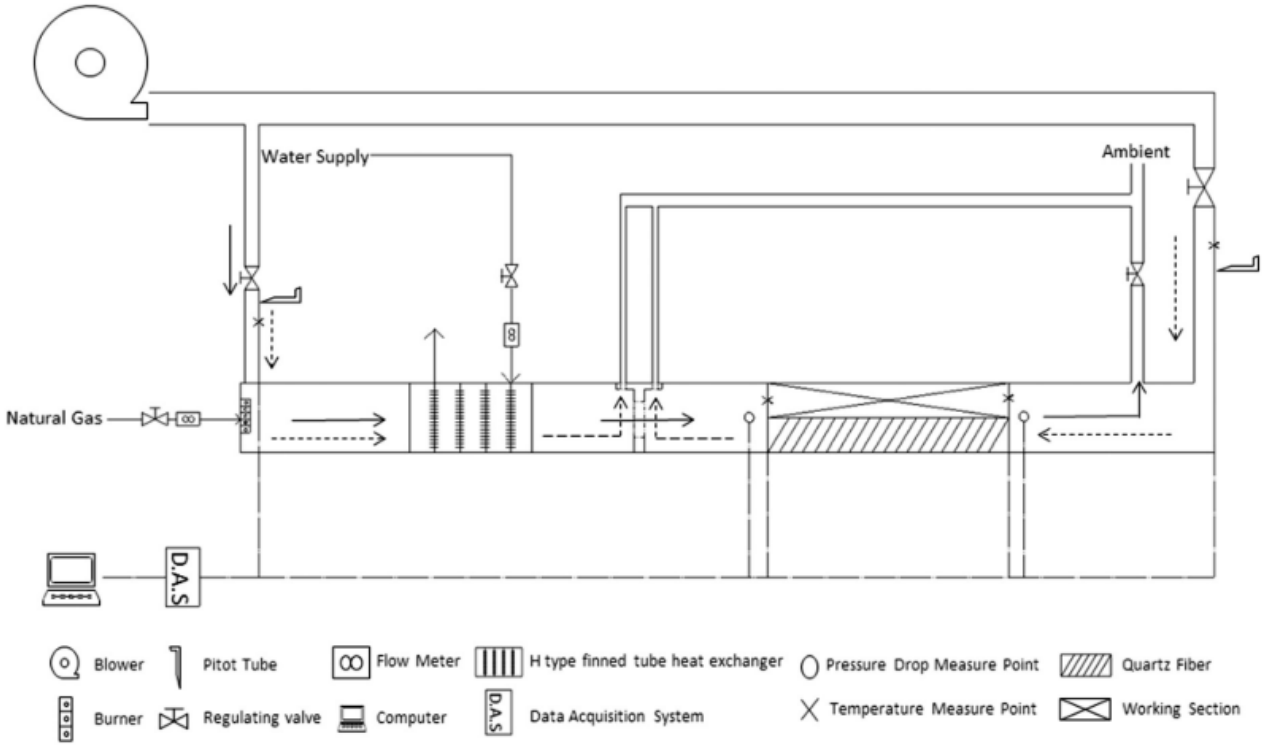


Figure 8. Schematic diagram of experimental system suggested by [31].

A failure cause analysis of heating elements was conducted by Shayan et al. [39]. Depositions, heating elements, and enamel coating were subjected to visual investigation, chemical analysis, and microscopic examination. As heating elements, two kinds of plates were utilized. The first is a corrosion-resistant low-alloy steel called Corten, the second material is enamel-coated basic carbon steel (also known as substrate). Because of sulfuric acid dew-point corrosion and under-deposit pitting corrosion, the heating elements failed (Figure 9). Iron sulfate, iron oxide, and iron sulfide were the most common corrosion products. In reality, corrosion issues at the power facility resulted from the usage of low-quality fuel. Choi et al.[40] have an experimental investigation to remove NO from the air preheater and exchange heat simultaneously, a parallel passage type reactor (PPR) consisting of a heating element with a V2O5-WO3/TiO2 catalyst coating has been created. The effectiveness of the heating element method in the air preheater for concurrently exchanging heat and eliminating NO as a PPR (parallel passage reactor). Because of the plate's thin layer of catalyst coating, the element exhibits good performance of NO removal activity together with no discernible change in heat transfer efficiency. Pongsaksawad and Kaewkumsai [41] stated that, according to the analytical data, the heating element with a higher silica concentration showed less damage overall. As more pores formed in the coating layer, the protective qualities of the coatings diminished. Less damage was done to the heating element that was covered in a coating of tougher porcelain. After investigating how enameling parameters affect fresh

porcelain-enamel coatings Cheli et al.[42] reported high resistance to acid corrosion, low bollosity (%), excellent mechanical properties, and strong adhesion to the substrate. The technique for utilizing the air heater as SCR reactor is described by Wejkowski and Wojnar Silesian[43] along with the anticipated advantages. Catalytic components serve as both heating surfaces and carriers of catalysts in this technique. Heat transfer and NOx reduction study of the catalytic elements is presented. Three types of catalysts were selected: one containing 0.5% of Cu and 1.5% of Mn, another containing 0.5% of Cu and 0.5% of Mn. A 40% decrease in NOx was the maximum that could be accomplished.

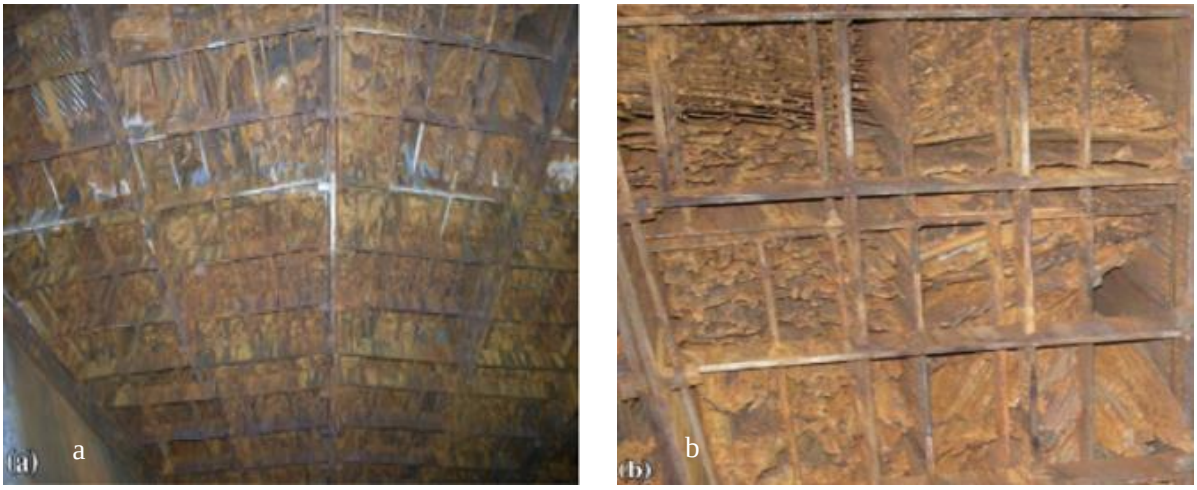


Figure 9. Heating element failure in an air heater setup: (a) bottom view of the baskets, and (b) failed heating elements in the baskets [32].

## 4. Configuration of flow

Subsequent industrial-scale studies highlighted the issue of leakage; for example, Drobnič et al. [44] analyzed leakage in a 275 MW air preheater, showing a 1.5–2% increase in $CO_2$ emissions in "leaky" versus "tight" operation. Further sealing strategies, such as the low-leakage system (LLS) studied by Wang [45], decreased leakage by 66% with only modest increases in pumping power. Similarly, leakage-focused CFD studies introduced by Zhu et al. [46] confirmed that optimized sealing geometries improved efficiency by about 6%. Results based on Akbari et al.[47] showed that the heat regeneration temperature and the heat exchanger's efficiency were shown to decline as the matrix's rotating speed and the hot flow's mass flow rate increased. The most useful metric for determining the efficiency and regeneration temperature was the inlet hot flow temperature. Furthermore, there was a nonlinear increase in the regeneration temperature and efficiency as the inlet hot flow temperature was raised. A modified single-blow technique was introduced and expressed by Butrymowicz et al. [48]. For the examined matrices of the regenerative gas heater, the exemplary dimensionless relationships between the Reynolds number, Darcy flow resistance factor, and Colburn heat transfer factor were shown. It was shown that the measured and theoretically predicted temperature profiles agreed. Figure 10 shows the schematic daigram of the experimental facility. Babu et al. [25] used (CFD- fluent) to run computational simulations of air passing over heat transfer elements with various configurations, such as a rectangular vortex generator, a trapezoidal vortex generator, an isosceles triangular vortex generator, and an inward line right angle triangle vortex generator. The thermal fatigue stress caused by the temperature difference between heating and chilling cycles has a negative impact on the overall efficiency of the metal matrix. In comparison to other types of vortex generators, the performance ratio of the rectangular type vortex generator is the highest, and its surface heat transfer coefficient is also the highest, tying it with the isosceles triangle type vortex generator. Various inlet conditions and flows result in a lower pressure decrease compared to other configurations. Patil et al. [9] determine the outflow temperatures of various profiles (CU, NF, NC, DU, and Advanced Clear Element (ACE)).

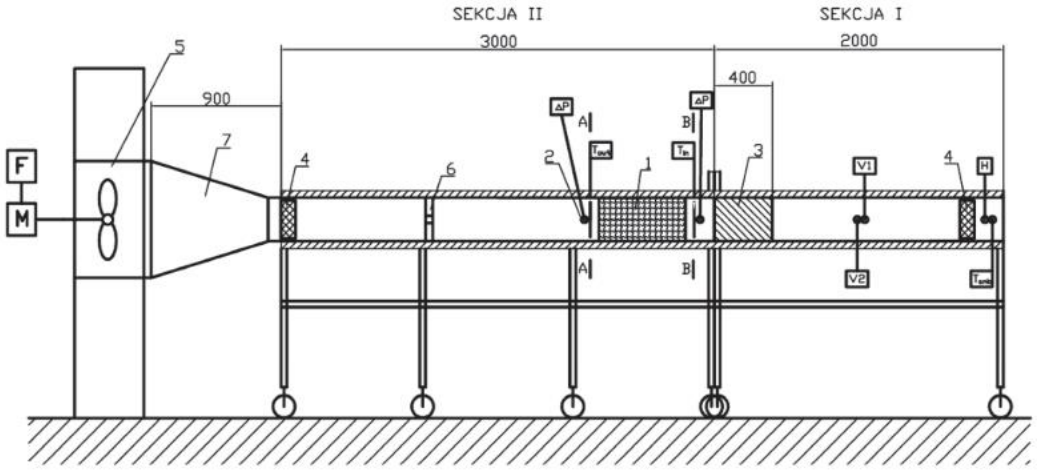


Figure 10. Schemtic daigram of the experemental facility suggested by [38]

The heat exchange of an air preheater is primarily determined by the element profile. Comparing the outlet temperature of heated flue gases and air, Advanced Clear Element (ACE) demonstrates favorable results. Wang et al. [49] used the finite difference approach to compute the temperature distribution of the matrix in an air preheater, and then used the finite element method to calculate the thermal stress-induced deformation based on the obtained temperature distribution. The effects of operating parameters, inlet-gas temperature, geometric parameters (including rotor radius and height), and sealing systems were investigated. The key findings were as follows:

Temperature distributions oriented axially were nonlinear on the matrix as well as the segmental plates. The existence of the gaps between the heat-transfer matrix layers significantly affected the temperature distribution on the segmental plate; therefore, these gaps must be accounted for when estimating the temperature of the segmental plate. The effect of $T_{g,in}$ on the temperature distribution decreased as the height coordinate decreased, while the effect of $T_{g,out}$ increased. At various tangential coordinates, the temperature distributions overall along the height coordinate were comparable and almost autonomous of the rotor's height. The aggregate temperature peaked at the interface between gases and air and dropped to its lowest point at the interaction of air and gas. The viability of the experiment system research on the heat transfer and flow characteristics is confirmed by an experiment by Jianqiang and Xingpeng [50] using NF heat transfer components to determine the convective heat transfer coefficient and resistance coefficient of this heat transfer element at varying wind speeds. The effect of increasing the primary air inlet opening, which minimizes the primary drop in air pressure across the air preheater, has been studied by Mohit Rajput [51] in order to overcome the high drop in pressure across the air preheater. As the primary air opening increases, the pressure drop across the air preheater's primary section is significantly reduced. The air preheater's thermal performance is enhanced by expanding the primary air opening. Du et al. [52] compared quad-sector to tri-sector RAPH designs, reporting a 33.1% reduction in leakage.

Chen et al.[53] primarily study the fly ash deposition characteristics on the heat transfer element's surface using a tiny simulated air preheater. The overall ash deposition intensity on the heat transfer element's plate surfaces steadily increases as the gas velocity drops. This is because fly ash particles have a longer residence period in the channel at lower gas velocities. This increases the likelihood that the fly ash particles will settle on the heat transfer elements' surfaces, increasing the total ash deposition intensity.
According to Zhang and Che [54] measured data, the performance of the DN plate is in between that of the cross-corrugated (CC) plate and the parallel plate, Figure 11, and it is similar to that of the double undulated (DU) plate. There is no discernible whirling flow pattern in the anticipated velocity fields. In essence, two

different forms of flow are seen: pipe flow and wavy channel flow. Undulations and notches on the luff or lee side yield high or low Nusselt numbers, Nu, respectively. As Reynolds numbers rise, Nu values rise and Nu distributions become more homogeneous. shows the experimental apparatus.

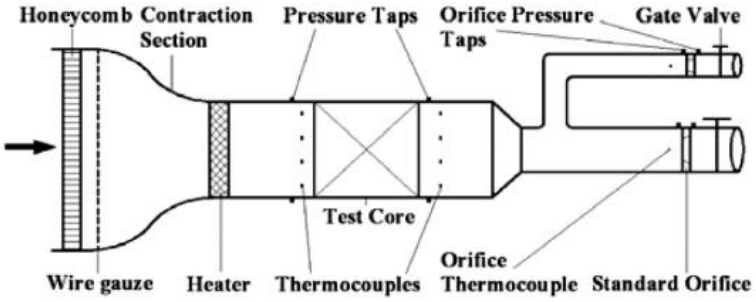


Figure 11. The experemental apparitus used in [43]

Usually, the air preheater receives the boiler combustion air at 600 K and allows it to cool down to 400 K. Figure 12 displays the temperature profile along the air preheater[55].

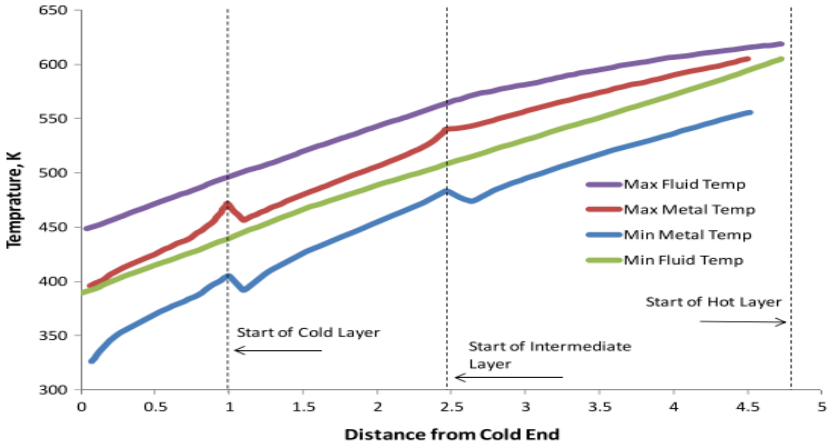


Figure 12. Temperature profile along a three layer air preheater [44]

A comparative analysis of the air and gas temperatures computed using the 1-D and 3-D models have been developed by Alagic et.al[56]. The regenerator's whole height is shown in the temperature distribution. A high degree of agreement is attained between the two models, yet the finest knowledge of the flow behavior is provided by the 3D model. In order to compare the outcomes of theoretical modeling with experimental data that was directly measured on a full-scale working air preheater, Skiepko and Shah[57] conducted a comparison. Data from experiments are compared with the estimated temperature distributions. Findings show that theory and experiments accord fairly well, with the right tendencies emerging.

Through the use of pin-shaped turbulators (promoters), a systematic artificial roughening of the heat transmission elements is studied by Al-Kayiem and Mahdi[58] in order to improve the system's performance. Based on efficiency index values, the results showed that artificial roughening by pins improved performance. When the pitch /pin-to-height ratio is 10, the results showed a larger augmentation. Most recently, Chen et al. [59] evaluated soot-blowing in 600 MW APHs, showing a 22% reduction in vibration amplitude and a 25% increase in cleaning coverage at full-load conditions

## 5. Mathematical relations

In this section, the fundamental mathematical relationships governing heat transfer and fluid flow in rotary air preheaters are presented. The purpose of including these formulations is not only to provide the theoretical basis of the study but also to serve as a useful reference for future researchers and engineers interested in analyzing or designing RAPH systems. Mathematical modeling offers a systematic framework to quantify parameters such as heat transfer coefficient, Nusselt number, friction factor, and thermal effectiveness, which are essential for predicting system performance under different operating conditions. Moreover, these relationships bridge experimental findings with computational fluid dynamics (CFD) simulations, enabling accurate validation and optimization of design parameters. By explicitly stating the governing equations and assumptions, this section ensures transparency, reproducibility, and comparability with other studies. Roșu and Ionel [60] emphasized that a Rothemuhler-type rotating-plate regenerative air preheater was suitable for validating mathematical models, since the choice between a mobile (Ljungström type) or stationary (Rothemuhler type) rotor had little influence on the temperature distribution of air and flue gases. This is mainly because the heat transfer process is governed more by the thermal mass and geometry of the metal filler than by the rotational speed. In practical terms, this finding highlights that both configurations can be reliably used for model verification, ensuring broader applicability of the mathematical formulations. While experimental techniques for determining heat transfer coefficients are often limited to indirect measurements such as evaluating inlet/outlet temperature differences along with flow rate, surface area, and density computational fluid dynamics (CFD) provides a more versatile approach. In CFD, the local heat transfer coefficient can be directly calculated through integrated functions, allowing not only for validation of theoretical models but also for practical design optimization. Thus, the mathematical relationships are not merely abstract, but serve as a basis for developing reliable predictive tools with direct implications for improving RAPH efficiency.

In the experimental calculation, the heat transfer rate can be found from the following equation [61].

$$Q = \dot{m} C_{p,air} (T_{in}^{'} - T_{out}^{'}) \quad (1)$$

The overall model's mean heat transfer coefficient is computed from Newton law of cooling [62].

$$h = \frac{q_{con}}{(T - T_{ref})} \quad (2)$$

A fluid boundary's ratio of convective to conductive heat transfer is known as the Nusselt number, and calculated by the equation [63].

$$Nu = \frac{hD_h}{k} \quad (3)$$

Where: hydraulic diameter is given by equation 3 [64].

$$D_h = \frac{4A}{P} \quad (4)$$

The Reynolds number is a representation of the fluid's inertial to viscous force ratio [65].

$$Re = \frac{\rho . u . D_h}{\mu} \quad (5)$$

The ratio of thermal diffusivity to momentum diffusivity is known as the Prandtl number [66].

$$Pr = \frac{\mu . C_p}{k} \quad (6)$$

The Colburn factor, J, is the relationship between mass transfer coefficients, heat transfer coefficients, and friction factor which measures efficiency per unit pressure drop [67].

$$J = \frac{Nu}{Re.Pr^{1/3}} \quad 7$$

The "friction factor" is used to calculate the pressure drop characteristics and it is given by Darcy equation [68].

$$f = \frac{2.\Delta p.D_h}{L.\rho_{air}.u^2} \quad 8$$

The ε-NTU technique for the design of a heat exchanger introduces the number of transfer units (NTU) and the effectiveness of heat transfer (ε) as two crucial criteria. This is how they are defined[69]:

$$\varepsilon = \frac{|T_{in}-T_{out}|max}{T_{g,in}-T_{a,in}} \quad 9$$

$$NTU = \frac{KA}{C_{min}} \quad 10$$

## 6. Heating elements specifications

The primary crucial factors of a Ljungström regenerative APH pertain to the heating element shape. In fact, they must be selected to enhance heat transfer, minimize pressure drop, and to ensure that the matrix can be cleaned, and the ashes removed[70]. Corten steel, also known as HSLA (High strength low alloy steel), is the material used to make the heating components in air preheaters. Because of its strong heat conductivity and high resilience to corrosion and erosion, corten steel is the material of choice for heating element. An air preheater's performance is also significantly impacted by the shape of the heating elements that are utilized. It is divided into eight familiar categories according to the profile as shown in Table 1

Table 1 Profile of the heating elements.

| Name of element | Symbol | Geometry | Reference |
|---|---|---|---|
| Double Undulated | DU | 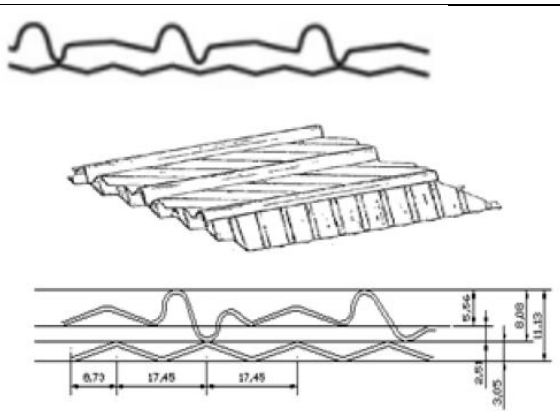 | S.Babu[71]<br><br>S. Vulloju [31] |

| | | | |
|---|---|---|---|
| Double Notched | DN |  | R.Raj and Modi et al. [5], [8] |
| Double Notched Loose Packed | DL |  | R.Raj and Modi et al. [5], [8] . |
| Flat Notched Crossed | FNC | 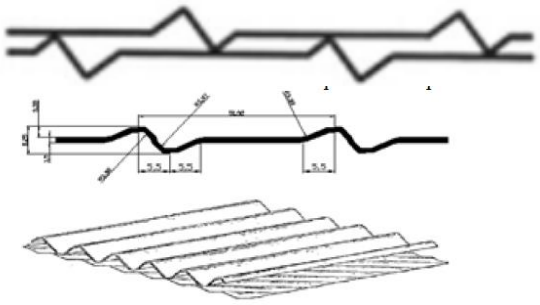 | R.Raj and Modi et al. [5], [8]<br>S. Vulloju[31] |
| Notched Flat | NF | 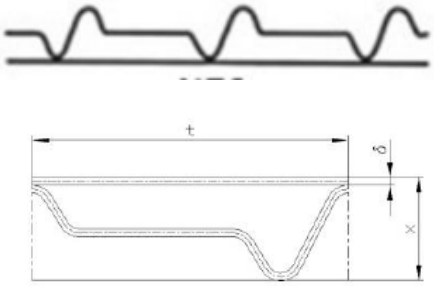 | R.Raj and Modi et al. [5], [8]<br>Stuper et al. [32] |
| Notched Undulated | NU |  | Modi et al. [8] |
| Corrugated Undulated | CU | 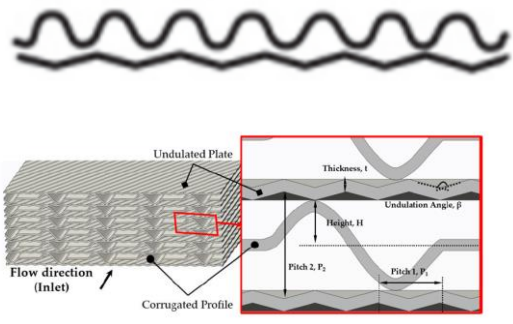 | R.Raj [5]<br>Modi et al. [8]<br>Lee et al. [12] |
| Advanced Clear Element | ACE |  | Patel et.al [7] |

According to their usage, heating elements can be classified into hot, intermediate, and cold layers. They differ in metal, profile and height. Although most researchers have reported that cold and intermediate layers are identical but R.Pachaiyappan and J. Dasa Prakash[72] showed that heating elements at hot end and intermediate end are the same. Table 2 shows the specifications of the three layers.

Table 2. Specifications of the three air pre heater layers

| Reference | Characteristics | Hot layer | Intermediate layer | Cold layer |
|---|---|---|---|---|
| Hajebzadeh and. Ansari[7] | Profile | DU | NF | NF |
| | Thickness(mm) | 0.6 | 0.6 | 1.25 |
| | Height(mm) | 762 | 438 | 305 |
| | Material | Mild steel | Mild steel | Corten steel |
| Zhang et al. [37] | Profile | DU | - | DU |
| | Thickness(mm) | 0.5 | - | 0.8 |
| | Height(mm) | 1200 | | 400 |
| Wang et al. [38] | Height(mm) | 450,300 | 900,300 | 700, 684 |
| | Heat transfer correlation | $Nu = 0.083Re^{0.69}pr^{0.4}$ | $Nu = 0.266Re^{0.55}pr^{0.4}$ | $Nu = 0.112Re^{0.641}pr^{0.4}$ |
| | Friction factor correlation | $f = 2.641Re^{-0.376}$ | $f = 8.488Re^{-0.538}$ | $f = 2.63Re^{-0.373}$ |
| Stupar et al. [32] | Profile | DU | DU | NF |
| | Thickness(mm) | 0.6 | 0.6 | 1 |
| | Height(mm) | 1400 | - | 300 |
| S.Babu et al. [71] | Profile | DU | DU | NF |
| | Thickness(mm) | - | - | 1.214 |
| | Height(mm) | - | - | 100 |
| Abroshan and Goodarzi [23] | Profile | DU | DU | NF |
| | Height(mm) | 800 | 450 | 305 |
| Bureska and Bundalevski [19] | Profile | DU | DU | NF |
| Shaya n et al. [39] | Profile | DU | DU | DU |
| | Height(mm) | 1250 | - | 650 |
| Hazem and Alhamdo[36] | Profile | CP | CP | Gravel |
| | Height(mm) | 500 | 350 | 150 |
| | Material | Carbon steel | Corten steel | Gravel |

Table 3. Summary of review papers investigated the performance of heating elements considering the statistical.

| **Paper (year)** | **Geometry / Conditions** | **Re range** | **Investigated parameters** | **Comparison aspects** | **Study outcomes** | **Porous media** |
|---|---|---|---|---|---|---|
| Stasiek (1995) [12] | Cross-corrugated | $10^2$-$10^4$ | Nu, $f$ | Exp. vs Num. models | LES best | No |
| Ciofalo et al. (1996) [13] | Cross-corrugated plates | $10^3$-$10^4$ | Nu, f | LES vs exp. | LES matched best | No |
| Alagić et al. (2005) [56] | Ljungström APH, 1D vs 3D model | – | T distribution error 0.8-6% | 1D vs 3D | Heat transfer ↑3.2% at 3 rpm | No |
| Choi et al. (2005) [40] | PPR catalyst | – | NO removal | PPR vs honeycomb | Predicted well | No |

| | | | | | | |
|---|---|---|---|---|---|---|
| Drobnič et al. (2006) [44] | 275 MW APH leakage | – | Tout, $CO_2$ fraction | Tight vs leaky | $CO_2$ ↑1.5-2% | No |
| Jain (2007) [73] | Small PHE, chevron | 400-1300 | Nu, f | Correlations vs exp. | Nu under by 13% | No |
| Skiepko (2004) [57] | 5.3 m APH | – | η ~88% | Model vs exp. | Error ≤7% | No |
| Ghodsipour (2003) [74] | Lab regenerator, triangular | 3000-10,000 | η | Exp. vs Num. | Thermal efficiency: 0.58-0.98 | Yes |
| Wang (2008) [75] | RAPH exergy | – | E, $Z_0$ | Ideal vs real | Opt. hot end ratio | No |
| Wang (2009) [34] | Stress, deformation | – | Δ, stress | Simplified vs exp. | Error 1-5% | No |
| Abdulsada & Alhamdo (2013) [30] | 13 matrix configs: corrugated plates, wire mesh, stone media | 680-10,100 | j-factor correlations | Corrugated vs wire and stone configurrations | Corrugated ↑25-30%, SWM ↑40%, small stone ↑70% | No |
| Sreedhar (2013) [31] | FNC vs DU, wind tunnel | 5k–50k | h, PP | FNC vs DU | PP ↓19.3% | No |
| Wei (2013) [22] | 2- vs 3-sector RAPH | – | Tout | Sim vs plant | Dev. ±5 °C | No |
| Zhang & Che (2012) [15] | Double notched plates | ~4700 | Nu, j, *f* | DN vs DU, CC | CFD dev ±17% | No |
| Zhang (2011) [54] | DU plate APH | – | Tout, ε | Exp. vs sim | Good match | No |
| Gao & Gu (2014) [50] | NF plates | 5–14 m/s | h, *f* | – | h↑0.036→0.050 | No |
| Maharaj (2015) [1] | Seal leakage, APH CFD | – | Leak mass flow | CFD vs exp. | CFD under by ~24% | Yes |
| Shayan (2015) [39] | DU-type APH, corrosion | – | ADPT, failure | ADPT vs CFD vs field | ADPT 138-142 °C | Yes |
| Corsini et al. (2015) [70] | 15 m RAPH, CFD | – | Tout, ΔP | CFD vs Enel exp. | Error ~3% | Yes |
| Menasha (2011) [55] | Bench ABS test | ~1600 | ABS T 500–520K | Prior studies | Good agreement | No |
| Wang (2015) [49] | FEM/FDM RAPH | – | Δ max. ~60 mm | FEM vs plant | Error <7% | No |
| Wang (2016) [28] | CU plates, SVR | 1.5k–10k | Nu, f | vs Stasiek exp. | Dev ±13% | No |
| Rajput (2016) [51] | Tri-sector RAPH CFD | – | ΔP, η, T | Angles, rpm | Opt. 70°, 2-3 rpm | Yes |
| Lee (2017) [27] | GGH, corrugated L-type | >2300 | h, $CR_2$, η | Base vs optimized | η ↑7.7% | Yes |
| Wang (2017) [38] | Exp APH ceramic vs metal | 1.5k–5.7k | Nu, *f*, ε | Metal vs ceramic | Metal ε ↑8.6% | No |
| Akbari et al. (2018) [47] | Food dryer regenerator, zigzag Al sheets | – | $H_{avg.}$ 38.9% | Effect of flow, T, speed | η ↑ with Tin, ↓ with speed/flow | No |
| Wejkowski (2018) [43] | CFD frost wheel | – | ε, frost area | – | ε ↑ with rpm | No |
| Bu et al. (2019) [17] | Split RAPH, DU vs DU3E | – | ε, ΔP, ABS | Split vs traditional | ABS ↓90%, payback <2 yr. | No |

| | | | | | | |
|---|---|---|---|---|---|---|
| Du et al. (2019) [52] | Quad vs tri RAPH | – | Leakage, Tout | Quad vs tri | Leakage ↓33.1% | Yes |
| Wang (2019) [26] | Tri-sector RAPH | – | ε, ΔP, weight | Pareto optimized | Weight ↓43% | No |
| Zhang (2019) [37] | 3-layer RAPH | – | ε, ΔP, ABS | Pareto optimized | Weight ↓30% | No |
| Hazim (2020) [36] | Exp. APH gravel + bypass | 25k–98k | $Q_{av.}$, PP, η | P matrix vs mods | $Q_{av.}$ ↑22%, η ↑ | Yes |
| Abroshan & Goodarzi (2020) [23] | 3-layer Ljungström RAH, CFD 13 passages | up to 10,000 | $Nu/f^{1/3}$, fuel saving | CU, DU, FNC profiles; plant validation | CU30 best; CFD overestimated Nu by 30-56% | No |
| Güllüce (2020) [20] | RHEX CU plates, NSGA-II | 1000–10,000 | ε, cost, entropy | Baseline vs optimized | ε ↑92%, cost ↓46% | No |
| Hajabdollahi (2020) [76] | Constructal rotary regenerator | – | ε, TAC | Constructal vs conventional | ε ↑7%, TAC ↓34% | No |
| Wang (2020) [45] | GGH with LLS | – | Leak, ε, PP | With vs without LLS | Leak ↓66%, PP ↓12kW | Yes |
| Zhu (2020) [46] | Leakage CFD | – | Tout, η | – | η ↑6% | Yes |
| Hajebzadeh (2021) [7] | 320 MW RAPH, DU+NF | 2500–6000 | η, Tout, leakage | Exp. vs CFD | η ↑6%, leakage ↓⅔ | Yes |
| Subramaniyan (2021) [6] | 250 MW APH, VFD | – | Q, η | Full vs part load | Opt. 62 MW | No |
| You (2021) [21] | Honeycomb vs DU | – | Nu, ΔP | Honeycomb vs DU | ΔP ↓10% | No |
| Babu et al. (2021) [71] | CFD, vortex generators vs NF | 2300–8000 | h, exit T, enthalpy | VG vs NF | Rectangular VG best | No |
| Chen et al. (2020) [53] | Tri-compartment APH | – | h, T distribution | Analytical vs numerical | Faster convergence, adaptable | No |
| Chen et al. (2023) | CU element, ABS deposition | – | Adhesion %, deposition | With vs without ABS | Max adhesion 31.7% | No |
| White (2023) [18] | New CFD soot model | – | Coverage, ΔT | – | Valid vs exp. | Yes |
| Chen et al. (2024)[59] | 600 MW APH soot-blowing | – | ΔV, ΔT, coverage % | Loads 300–600 MW | V ↓22%, coverage ↑25% | Yes |

## 7. Conclusions and future work

This review has included some essential details and perspectives about heating elements in the rotary air preheater. This paper's major contribution is offering an opinion regarding the effect of heating elements on the performance of air preheater working principle and further enhancements to increase the heat transfer rate, decrease pressure drop and maintain low fouling. A summary of the review papers are given in Table 3 which summarizes the results and the heating elements profile in addition to the papers method. The effect of element surface, material, and configuration on the flux of heating element in the APH is the focus of this study. Additionally, the research work includes the mathematical relations and heat transfer correlations used to analyze the performance of the heating elements. The notable improvement is the usage of FNC profile in the cold layer since these plates have a smaller pressure drop and better thermal performance. While, in hot and intermediate layers, DU utilized in high fouling applications because cleaning some parts of it is easy.

Further improvement on heating elements can be made using different material to resist corrosion or changing the profile dimension to enhance heat transfer. Also, the effect of the wall of the basket on the temperature distribution in the heating elements doesn't take in account in the most studies. Also, future studies should explore the use of Artificial Intelligence (AI) and Machine Learning (ML) to optimize the design of rotary air preheater elements, particularly in predicting and improving the balance between heat transfer and pressure drop. AI/ML can accelerate the design process by identifying optimal corrugation profiles and flow arrangements from large CFD and experimental datasets. At the same time, the development of hybrid materials-combining metals with ceramics, composites, or coatings-offers opportunities to enhance thermal performance, reduce fouling, and increase durability.

**Author Contributions:** The authors contributed to all parts of the current study.

**Funding:** This study received no external funding.

**Conflicts of Interest:** The authors declare no conflict of interest.

**Nomenclature**

**Symbols**

| | |
|---|---|
| A | area ($m^2$) |
| $C_{min}$ | the air and flue gas minimum heat capacity rate |
| Cp | specific heat (j /$kg{\cdot}K$) |
| Dh | hydraulic diameter ($m$) |
| h | coefficient of heat transfer ($W/m^2{\cdot}K$) |
| Hu | wave height of the plate, mm |
| k | thermal conductivity ($W/m{\cdot}K$). |
| NTU | Number of transfer units dimensionless |
| P | wetted Perimeter (m). |
| Pr | Prandtl number dimensionless |
| Pu | wave pitch of the plate, mm |
| Q | Heat transfer rate (w) |
| q | heat flux at the boundary ($W/m^2$) |
| $\Delta P$ | pressure drop (Pa) |
| $L$ | length ($m$) |
| $Nu$ | Nusselt number dimensionless |
| $Re$ | Reynolds number dimensionless |
| $T$ | temperature ($K$) |
| $f$ | friction factor dimensionless |
| $u$ | velocity ($m/s$) |
| **Greek symbols** | |
| ε | the effectiveness of heat transfer |
| η | thermal efficiency |
| $\mu$ | dynamic viscosity ($Pa{\cdot}s$). |
| $\rho$ | density ($kg/m^3$) |
| **Abbreviations** | |
| ACE | advanced clear element |

| | |
|---|---|
| ADPT | acid dew-point temperature |
| AI | artificial Intelligence |
| Av. | average |
| CC | Cross corrugated |
| CFD | computational fluid dynamics |
| CP | Corrugated plate |
| CRLS | corrosion-resistant low-alloy steel |
| $C_{R2}$ | Quadratic resistance coefficient($kg/m^4$) |
| CTPPs | coal-fired thermal power plants |
| CU | Corrugated undulated |
| DEV. | deviation |
| DN | Double notched |
| DU | Double undulated |
| Exp. | experimental |
| FAHP | fuzzy analytic hierarchy process |
| FDEMATEL | fuzzy decision-making and trial laboratory |
| FDM | finite difference method |
| FEM | finite element method |
| FNC | Flat notched corrugated |
| FP | Flat plate |
| GGHs | gas-gas heaters |
| HSLA | high strength low alloy steel |
| LES | large turbulent eddies |
| LLS | low-leakage system |
| ML | machine Learning |
| NC | Notched corrugated |
| NF | Notched flat |
| Num. | numerical |
| Opt. | optimum |
| P matrix | standard air preheater matrix |
| P+CG | the corrugated plates with gritty gravel in the modified matrix |
| P+CG+Ti | corrugated plates with coarse gravel and bypass insertion |
| P+CG+Ts | corrugated plates with coarse gravel in staggered |
| PEEK | polyether ether ketone |
| pp | Pumping power |
| PPR | parallel passage type reactor |
| PTFE | Polytetra fluoro ethylene |
| RAPH | Regenerative Air Preheater |
| RHEX | Rotary regenerative heat exchanger geometry |
| RRs | rotary regenerators |
| RSM | response Surface Methodology |
| SWM | Staggered wire mesh |
| TAC | total annual cost |
| Yr. | year |

Subscripts

| | |
|---|---|
| a | air |
| cond. | conduction |
| g | gas |
| in | inlet |

| | |
|---|---|
| max. | maximum |
| min. | minimum |
| out | outlet |
| Ref. | reference |
| u | undulation |

**References**

[1] A. Maharaj, W. Schmitz, and R. Naidoo, "A numerical study of air preheater leakage," *Energy*, vol. 92, pp. 87–99, 2015, doi: 10.1016/j.energy.2015.06.069.

[2] L. B. M. Van Kessel, A. R. J. Arendsen, P. D. M. De Boer-Meulman, and G. Brem, "The effect of air preheating on the combustion of solid fuels on a grate," *Fuel*, vol. 83, no. 9, pp. 1123–1131, 2004, doi: 10.1016/j.fuel.2003.11.008.

[3] V. Kumhar, V. Borkar, S. Imam, and P. G. Scholar, "Optimization of Heat Transfer Coefficient of Air Preheater using Computational Fluid Dynamics," *IJSRD-International J. Sci. Res. Dev.*, vol. 4, no. 05, pp. 2321–0613, 2016, [Online]. Available: www.ijsrd.com

[4] L. Liu and L. Zou, "The present situation and the future of air preheater in power," no. Icmemtc, pp. 385–389, 2016, doi: 10.2991/icmemtc-16.2016.74.

[5] R. Raj, "Numerical Analysis of Rotary Air-Preheater for Different Operating Conditions," vol. 10, no. 05, pp. 62–68, 2021.

[6] J. Subramaniyan and S. Venkatachalapathy, "Heat transfer studies at different speeds and loads of regenerative air preheater in thermal power plant," *Therm. Sci. Eng. Prog.*, vol. 22, no. December 2020, p. 100814, 2021, doi: 10.1016/j.tsep.2020.100814.

[7] H. Hajebzadeh and A. N. M. Ansari, "Modification of rotary air preheater toward achieving extended life-span utilizing porous media approach: A case study," *Proc. Inst. Mech. Eng. Part A J. Power Energy*, vol. 236, no. 2, pp. 293–307, 2022, doi: 10.1177/09576509211034977.

[8] A. Modi *et al.*, "A Review on Air Preheater Elements Design and Testing To cite this version : HAL Id : hal-01966399," 2018, doi: 10.2412/mmse.86.90.615.

[9] D. S. Patel, M. D. Patel, and S. A. Thakkar, "Numerical Analysis of Rotary Air Preheater : a Review," pp. 2496–2499, 2015.

[10] Abhijit Rajan, Suresh Kumar Badholiya, and Rohit Kumar Choudhary, "A Review Paper on CFD Analysis of Tri-sector Air Preheater for different Primary Air Inlet Opening," *Int. J. Eng. Res.*, vol. V6, no. 06, pp. 982–984, 2017, doi: 10.17577/ijertv6is060459.

[11] N. Baruah and K. G. V. Prasanna, "Numerical Modeling of Regenerative Rotary Heat Exchanger: A Review," *J. Biosyst. Eng.*, vol. 42, no. 1, pp. 44–55, 2017, doi: 10.5307/jbe.2017.42.1.044.

[12] J. A. Stasiek, "Experimental studies of heat transfer and fluid flow across corrugated-undulated heat exchanger surfaces," *Int. J. Heat Mass Transf.*, vol. 41, no. 6–7, pp. 899–914, 1998, doi: 10.1016/S0017-9310(97)00168-3.

[13] M. Ciofalo, J. Stasiek, and M. W. Collins, "Investigation corrugated of flow and heat transfer Numerical simulations," *Int. J. Heat Mass Transf.*, vol. 39, no. 1, pp. 165–192, 1996.

[14] N. Ghodsipour and M. Sadrameli, "Experimental and sensitivity analysis of a rotary air preheater for

the flue gas heat recovery," *Appl. Therm. Eng.*, vol. 23, no. 5, pp. 571–580, 2003, doi: 10.1016/S1359-4311(02)00226-0.

[15] L. Zhang and D. Che, "Influence of corrugation profile on the thermalhydraulic performance of cross-corrugated plates," *Numer. Heat Transf. Part A Appl.*, vol. 59, no. 4, pp. 267–296, 2011, doi: 10.1080/10407782.2011.540963.

[16] T. Sivageerthi, B. Sankaranarayanan, S. M. Ali, and K. Karuppiah, "Modelling the Relationships among the Key Factors Affecting the Performance of Coal-Fired Thermal Power Plants: Implications for Achieving Clean Energy," *Sustain.*, vol. 14, no. 6, pp. 1–28, 2022, doi: 10.3390/su14063588.

[17] Y. Bu, L. Wang, L. Deng, and D. Che, "Technical and economical analysis of a novel rotary air preheater system," *Appl. Therm. Eng.*, vol. 154, no. November 2018, pp. 102–110, 2019, doi: 10.1016/j.applthermaleng.2019.03.007.

[18] J. White and M. Vezza, "Multi-Objective Optimisation of Heat Transfer Elements within A Rotary Regenerative Heater," *Proc. 8th World Congr. Momentum, Heat Mass Transf.*, pp. 1–11, 2023, doi: 10.11159/enfht23.173.

[19] L. J. Bureska and S. Bundalevski, "The Improvement A Sealing of the Regenerative Air Preheaters of the Coal Boiler and Its Effect on Boiler Efficiency," vol. 4, no. 3, pp. 13–20, 2022, doi: 10.35629/5252-04031320.

[20] H. Güllüce and K. Özdemir, "Design and operational condition optimization of a rotary regenerative heat exchanger," *Appl. Therm. Eng.*, vol. 177, no. March, p. 115341, 2020, doi: 10.1016/j.applthermaleng.2020.115341.

[21] Y. Yu, H. Di, B. Zhao, and H. Li, "Analysis of influence of ripple parameters of heat storage elements on flow and heat transfer performance," *Therm. Sci. Eng.*, vol. 4, no. 2, p. 54, 2021, doi: 10.24294/tse.v4i2.1519.

[22] R. G. Wei, Z. X. Qu, and J. Q. Gao, "Heat exchange calculation of a regenerative air heater with numerical simulation method," *Adv. Mater. Res.*, vol. 860–863, pp. 1416–1419, 2014, doi: 10.4028/www.scientific.net/AMR.860-863.1416.

[23] H. Abroshan and M. Goodarzi, "Optimization of a three-layer rotary generator using genetic algorithm to minimize fuel consumption," *J. Mech. Eng. Sci.*, vol. 14, no. 1, pp. 6304–6321, 2020, doi: 10.15282/jmes.14.1.2020.09.0494.

[24] V. Patil and M. C. Navindgi, "Optimization and CFD Analysis on Profile Elements of Regenerative Rotary Air-Preheater," pp. 516–519, 2019.

[25] J. Manivel, L. Manimaran, M. Thiyagarajan, and P. Satheeshkumar, "Performance Analysis of Air Preheater in 210mw Thermal Power Station," *Internatinal J. og Adv. Res. Ideas Innov. Technol.*, vol. 3, pp. 619–630, 2017.

[26] L. Wang, Y. Bu, D. Li, C. Tang, and D. Che, "Single and multi-objective optimizations of rotary regenerative air preheater for coal-fired power plant considering the ammonium bisulfate deposition," *Int. J. Therm. Sci.*, vol. 136, no. September 2018, pp. 52–59, 2019, doi: 10.1016/j.ijthermalsci.2018.10.005.

[27] Y. M. Lee, H. Chung, S. H. Kim, H. S. Bae, and H. H. Cho, "Optimization of the heating element in a gas-gas heater using an integrated analysis model," *Energies*, vol. 10, no. 12, 2017, doi:

10.3390/en10121932.

[28] L. Wang, L. Deng, C. Ji, E. Liang, C. Wang, and D. Che, "Multi-objective optimization of geometrical parameters of corrugated-undulated heat transfer surfaces," *Appl. Energy*, vol. 174, pp. 25–36, 2016, doi: 10.1016/j.apenergy.2016.04.079.

[29] V. Mallikarjuna, N. Jashuva, and B. R. B. Reddy, "Improving Boiler Efficiency By Using Air Preheater," *Int. J. Adv. Res. Eng. Appl. Sci.*, vol. 3, no. 2, pp. 11–24, 2014.

[30] M. H. Alhamdo, "ES2013-18058 ENHANCEMENT PERFORMANCE OF ROTARY AIR PREHEATER FOR THERMAL POWER," pp. 1–10, 2013.

[31] S. Vulloju, "Analysis of Performance of Ljungstrom Air Preheater Elements," *Int. J. Curr. Eng. Technol.*, vol. 2, no. 2, pp. 501–505, 2013, doi: 10.14741/ijcet/spl.2.2014.94.

[32] G. Stupar, T. Zivanovic, D. Tucakovic, and M. Banjac, "Work optimization for rotary regenerative air preheater based on an increase of heat capacity of the matrix and reduction of leakage in seal clearances," *Proc. 26th Int. Conf. Effic. Cost, Optim. Simul. Environ. Impact Energy Syst. ECOS 2013*, no. July 2013, 2013, doi: 10.13140/2.1.3786.2722.

[33] H. Hajabdollahi and M. Shafiey Dehaj, "Rotary regenerator: Constructal thermoeconomic optimization," *J. Taiwan Inst. Chem. Eng.*, vol. 113, pp. 231–240, 2020, doi: 10.1016/j.jtice.2020.08.020.

[34] H. Y. Wang, X. L. Bi, L. L. Zhao, Q. T. Zhou, H. T. Kim, and Z. G. Xu, "A study on thermal stress deformation using analytical methods based on the temperature distribution of storage material in a rotary air-preheater," *Appl. Therm. Eng.*, vol. 29, no. 11–12, pp. 2350–2357, 2009, doi: 10.1016/j.applthermaleng.2008.11.022.

[35] T. T. Ngo, N. V. Nguyen, and D. W. Oh, "Analysis of the thermal performance of a flat-plate type rotary regenerator depending on the matrix material," *Int. J. Heat Mass Transf.*, vol. 189, p. 122728, 2022, doi: 10.1016/j.ijheatmasstransfer.2022.122728.

[36] S. M. Hazim and M. H. Alhamdo, "Performance Enhancement for Rotary Air Preheater of a Thermal Power Plant," *J. Eng. Sustain. Dev.*, vol. 24, no. 6, pp. 57–67, 2020, doi: 10.31272/jeasd.24.6.5.

[37] Q. Zhang, F. Sun, and C. Chen, "Research on the three-dimensional wall temperature distribution and low-temperature corrosion of quad-sectional air preheater in larger power plant boilers," *Int. J. Heat Mass Transf.*, vol. 128, pp. 739–747, 2019, doi: 10.1016/j.ijheatmasstransfer.2018.09.006.

[38] E. Wang, K. Li, J. Mao, N. Husnain, D. Li, and W. Wu, "Experimental study of flow and heat transfer in rotary air preheaters with honeycomb ceramics and metal corrugated plates," *Appl. Therm. Eng.*, vol. 130, pp. 1549–1557, 2018, doi: 10.1016/j.applthermaleng.2017.11.108.

[39] M. R. Shayan, K. Ranjbar, E. Hajidavalloo, and A. Heidari Kydan, "On the Failure Analysis of an Air Preheater in a Steam Power Plant," *J. Fail. Anal. Prev.*, vol. 15, no. 6, pp. 941–951, 2015, doi: 10.1007/s11668-015-0041-6.

[40] J. H. Choi, M. H. Kim, and I. S. Nam, "Heating element of an air preheater in a utility boiler as an SCR reactor removing NO by NH3," *Ind. Eng. Chem. Res.*, vol. 44, no. 4, pp. 707–714, 2005, doi: 10.1021/ie0492653.

[41] W. Pongsaksawad, S. Kaewkumsai, S. Sorachot, and E. Viyanit, "Failure of porcelain coated heating

elements used in regenerative air preheaters," *Mater. Test.*, vol. 57, no. 3, pp. 185–191, 2015, doi: 10.3139/120.110701.

[42] "Composite Enameled Steel Elements for Air Preheaters and Gas-Gas Heaters : an Integrated Approach From Sheet Forming and Enamelling," pp. 125–154.

[43] R. Wejkowski and W. Wojnar, "Selective catalytic reduction in a rotary air heater (RAH-SCR)," *Energy*, vol. 145, pp. 367–373, 2018, doi: 10.1016/j.energy.2017.12.077.

[44] B. Drobnič, J. Oman, and M. Tuma, "A numerical model for the analyses of heat transfer and leakages in a rotary air preheater," *Int. J. Heat Mass Transf.*, vol. 49, no. 25–26, pp. 5001–5009, 2006, doi: 10.1016/j.ijheatmasstransfer.2006.05.027.

[45] L. Wang, D. Li, H. Zhu, G. Chen, H. Luo, and D. Che, "Investigation on regenerative heat exchanger with novel low-leakage system for flue gas denitration in steel industry," *Appl. Therm. Eng.*, vol. 178, no. December 2019, p. 115483, 2020, doi: 10.1016/j.applthermaleng.2020.115483.

[46] D. C. Li, H. Zhu, L. M. Wang, Y. He, Y. F. Bu, and D. F. Che, "Experimental and Numerical Study on Direct Leakage of Rotary Air Preheater," *K. Cheng Je Wu Li Hsueh Pao/Journal Eng. Thermophys.*, vol. 41, no. 6, pp. 1325–1331, 2020.

[47] A. Akbari, S. Kouravand, and G. Chegini, "Experimental analysis of a rotary heat exchanger for waste heat recovery from the exhaust gas of dryer," *Appl. Therm. Eng.*, vol. 138, pp. 668–674, 2018, doi: 10.1016/j.applthermaleng.2018.04.103.

[48] D. Butrymowicz *et al.*, "Methodology of heat transfer and flow resistance measurement for matrices of rotating regenerative heat exchangers," *Chem. Process Eng. - Inz. Chem. i Proces.*, vol. 37, no. 3, pp. 341–358, 2016, doi: 10.1515/cpe-2016-0028.

[49] L. Wang, L. Deng, C. Tang, Q. Fan, C. Wang, and D. Che, "Thermal deformation prediction based on the temperature distribution of the rotor in rotary air-preheater," *Appl. Therm. Eng.*, vol. 90, pp. 478–488, 2015, doi: 10.1016/j.applthermaleng.2015.07.021.

[50] J. Q. Gao and X. P. Gu, "The experimental system design on heat transfer and flow characteristics of rotary air preheater," *Appl. Mech. Mater.*, vol. 602–605, pp. 90–93, 2014, doi: 10.4028/www.scientific.net/AMM.602-605.90.

[51] M. T. Disserttion, "Optimization of Primary Air Inlet Opening of Tri-Sector Air Pre-Heater for Minimising Primary Air Pressure Drop in Air Pre Heater (Aph) & To Study the Effect of Variation of Rpm on Aph Performance Using Cfd Analysis," no. June, 2016.

[52] X. Du, Y. Shi, and X. Wang, "Coupled characterization and experimental verification of heat transfer and air leakage in a quad-sectional rotary air preheater," *Appl. Therm. Eng.*, vol. 159, no. March, p. 113923, 2019, doi: 10.1016/j.applthermaleng.2019.113923.

[53] X. Chen, X. Ji, J. Feng, L. Heng, and L. Zhao, "Laboratory Study on Adhesive Ash Deposition Characteristics of Ammonium Bisulfate in Conditions Simulating an Air Preheater for Hard Coal Combustion," *Energies*, vol. 16, no. 18, 2023, doi: 10.3390/en16186513.

[54] L. Zhang and D. Che, "An experimental and numerical investigation on the thermal-hydraulic performance of double notched plate," *J. Heat Transfer*, vol. 134, no. 9, pp. 1–7, 2012, doi: 10.1115/1.4006210.

[55] J. Menasha, D. Dunn-Rankin, L. Muzio, and J. Stallings, "Ammonium bisulfate formation temperature in a bench-scale single-channel air preheater," *Fuel*, vol. 90, no. 7, pp. 2445–2453, 2011, doi: 10.1016/j.fuel.2011.03.006.

[56] S. Alagić, N. Stošić, A. Kovačević, and I. Buljubašić, "Numerical analysis of heat transfer and fluid flow in rotary regenerative air pre-heaters," *Stroj. Vestnik/Journal Mech. Eng.*, vol. 51, no. 7–8, pp. 411–417, 2005, doi: 10.1615/ichmt.2004.intthermscisemin.580.

[57] T. Skiepko and R. K. Shah, "A comparison of rotary regenerator theory and experimental results for an air preheater for a thermal power plant," *Exp. Therm. Fluid Sci.*, vol. 28, no. 2–3, pp. 257–264, 2004, doi: 10.1016/S0894-1777(03)00048-7.

[58] H. H. Al-Kayiem and H. A. A. Mahdi, "Performance enhancement of rotary air preheater by the use of pin shaped turbulators," *WIT Trans. Eng. Sci.*, vol. 68, pp. 35–49, 2010, doi: 10.2495/HT100041.

[59] Y. Chen, Y. Wang, B. Chen, H. Zhu, and L. Zhao, "Numerical Simulation Study on Rotary Air Preheater Considering the Influences of Steam Soot Blowing," *Energies*, vol. 17, no. 18, 2024, doi: 10.3390/en17184618.

[60] I. Roşu and I. G. Pîşă, "Numerical solution for the equation system that mathematically describes the heat transfer in a rotating- plate regenerative air preheater of a steam generator," *UPB Sci. Bull. Ser. D Mech. Eng.*, vol. 79, no. 3, pp. 35–48, 2017.

[61] R. Abou khachfe and Y. Jarny, "Determination of heat sources and heat transfer coefficient for two-dimensional heat flow – numerical and experimental study," *Int. J. Heat Mass Transf.*, vol. 44, no. 7, pp. 1309–1322, 2001, doi: https://doi.org/10.1016/S0017-9310(00)00186-1.

[62] S. Maruyama and S. Moriya, "Newton's Law of Cooling: Follow up and exploration," *Int. J. Heat Mass Transf.*, vol. 164, p. 120544, 2021, doi: https://doi.org/10.1016/j.ijheatmasstransfer.2020.120544.

[63] C. Yang, W. Li, and A. Nakayama, "Convective heat transfer of nanofluids in a concentric annulus," *Int. J. Therm. Sci.*, vol. 71, pp. 249–257, 2013, doi: https://doi.org/10.1016/j.ijthermalsci.2013.04.007.

[64] Y. Xu, "Calculation of unsaturated hydraulic conductivity using a fractal model for the pore-size distribution," *Comput. Geotech.*, vol. 31, no. 7, pp. 549–557, 2004, doi: https://doi.org/10.1016/j.compgeo.2004.07.003.

[65] G. Schewe, "Reynolds-number-effects in flow around a rectangular cylinder with aspect ratio 1:5," *J. Fluids Struct.*, vol. 39, pp. 15–26, 2013, doi: https://doi.org/10.1016/j.jfluidstructs.2013.02.013.

[66] S. J. Kim and S. P. Jang, "Effects of the Darcy number, the Prandtl number, and the Reynolds number on local thermal non-equilibrium," *Int. J. Heat Mass Transf.*, vol. 45, no. 19, pp. 3885–3896, 2002, doi: https://doi.org/10.1016/S0017-9310(02)00109-6.

[67] Z. Astolfi-Filho, E. B. de Oliveira, J. S. dos Reis Coimbra, and J. Telis-Romero, "Friction factors, convective heat transfer coefficients and the Colburn analogy for industrial sugarcane juices," *Biochem. Eng. J.*, vol. 60, pp. 111–118, 2012, doi: https://doi.org/10.1016/j.bej.2011.10.011.

[68] Z. Farmani, R. Azin, R. Fatehi, and M. Escrochi, "Analysis of Pre-Darcy flow for different liquids and gases," *J. Pet. Sci. Eng.*, vol. 168, pp. 17–31, 2018, doi: https://doi.org/10.1016/j.petrol.2018.05.004.

[69] B. Jayaraman and W. Shyy, "Modeling of dielectric barrier discharge-induced fluid dynamics and heat transfer," *Prog. Aerosp. Sci.*, vol. 44, no. 3, pp. 139–191, 2008, doi: https://doi.org/10.1016/j.paerosci.2007.10.004.

[70] A. Corsini, G. Delibra, G. Di Meo, M. Martini, F. Rispoli, and A. Santoriello, "A CFD-based virtual test-rig for rotating heat exchangers," *Energy Procedia*, vol. 82, pp. 245–251, 2015, doi: 10.1016/j.egypro.2015.12.029.

[71] B. S, D. V, K. Rajagopal, and G. M, "Air Preheater Temperature Analyses on Notched Flat Elementusing CFD," pp. 3–8, 2022, doi: 10.4108/eai.7-12-2021.2314548.

[72] R. Pachaiyappan and J. Dasa Prakash, "Improving the Boiler Efficiency by Optimizing the Combustion Air," *Appl. Mech. Mater.*, vol. 787, pp. 238–242, 2015, doi: 10.4028/www.scientific.net/amm.787.238.

[73] S. Jain, A. Joshi, and P. K. Bansal, "A new approach to numerical simulation of small sized plate heat exchangers with chevron plates," *J. Heat Transfer*, vol. 129, no. 3, pp. 291–297, 2007, doi: 10.1115/1.2430722.

[74] N. Ghodsipour and M. Sadrameli, "Experimental and sensitivity analysis of a rotary air preheater for the flue gas heat recovery," *Appl. Therm. Eng.*, vol. 23, no. 5, pp. 571–580, 2003, doi: https://doi.org/10.1016/S1359-4311(02)00226-0.

[75] H. Y. Wang, L. L. Zhao, Q. T. Zhou, Z. G. Xu, and H. T. Kim, "Exergy analysis on the irreversibility of rotary air preheater in thermal power plant," *Energy*, vol. 33, no. 4, pp. 647–656, 2008, doi: 10.1016/j.energy.2007.11.011.

[76] H. Hajabdollahi and M. Sha, "Journal of the Taiwan Institute of Chemical Engineers Rotary regenerator : Constructal thermoeconomic optimization," vol. 113, 2020, doi: 10.1016/j.jtice.2020.08.020.